Comparison of aberrations after standard and customized refractive surgery

L. Fang
fanglh71@126.com
Key Laboratory of Nondestructive Test (Ministry of Education), Nanchang Hangkong University, Nanchang, 330063, China

X. He
Key Laboratory of Nondestructive Test (Ministry of Education), Nanchang Hangkong University, Nanchang, 330063, China

Y. Wang
Tianjin Eye Hospital & Eye Institute, Ophthalmology and Visual Development Key Laboratory, Tianjin Medical University, Tianjin, 300020, China

To detect possible differences in residual wavefront aberrations between standard and customized laser refractive surgery based on mathematical modeling, the residual optical aberrations after conventional and customized laser refractive surgery were compared according to the ablation profile with transition zone. The results indicated that ablation profile has a significant impact on the residual aberrations. The amount of residual aberrations for conventional correction is higher than that for customized correction. Additionally, the residual aberrations for high myopia eyes are markedly larger than those for moderate myopia eyes. For a 5 mm pupil, the main residual aberration term is coma and yet it is spherical aberration for a 7 mm pupil. When the pupil diameter is the same as optical zone or greater, the magnitudes of residual aberrations is obviously larger than that for a smaller pupil. In addition, the magnitudes of the residual fifth or sixth order aberrations are relatively large, especially secondary coma in a 6 mm pupil and secondary spherical aberration in a 7 mm pupil. Therefore, the customized ablation profile may be superior to the conventional correction even though the transition zone and treatment decentration are taken into account. However, the customized ablation profile will still induce significant amount of residual aberrations.
[DOI: http://dx.doi.org/10.2971/jeos.2013.13061]

Keywords: Wavefront aberration, ablation profile, refractive surgery, myopia, optical quality

1 INTRODUCTION

Conventional laser refractive surgeries aim to correct the refractive errors of defocus and astigmatism based on the Munnerlyn formula. In addition, customized laser refractive surgery can be based on corneal topography or wavefront aberrations for correcting refractive errors. Wavefront-guided surgeries aim to address the total ocular wavefront aberrations in addition to the refractive errors [1, 2]. This paper concerns the comparison of postoperative wavefront aberrations for conventional and wavefront-guided corneal ablation.

Different ablation profiles may achieve statistically significantly different outcomes depending on refractive, patient, and laser platforms. Du *et al.* found that higher order aberrations were increased, but the increase of higher order aberrations after customized ablation treatment was less than that after conventional ablation [3]. Schallhorn *et al.* indicated that wavefront-guided myopia LASIK combined with a femtosecond laser flap significantly improved mean night driving visual performance and was significantly better than conventional LASIK using a mechanical keratome [4]. Awwad *et al.* showed that wavefront-guided ablation was associated with higher surgically induced astigmatism and larger astigmatic axis shift on the VISX platform as compared to the LADAR CustomCornea and the LADAR and VISX conventional platforms [5]. Zhang *et al.* reported that wavefront-guided LASIK with iris-registration was efficient to reduce higher order aberrations especially spherical and coma aberrations, and to improve postoperative visual acuity and contrast sensitivity compared with the conventional LASIK [6]. For the consideration of effective optical zone, a study demonstrated that CustomVue LASIK created larger corneal topographic effective optical zones than standard ablation [7]. The treatment decentration in laser refractive surgery has been observed in previous studies [8] and the results indicated that the centration errors had an important impact on the postoperative optical aberrations [9]. Therefore, decentration would be considered by Monte Carlo simulation. In our study, the use of a simulation procedure to generate a probability distribution of treatment decentrations was of great interest for several applications. Particularly, it may help understand the consequences of laser refractive surgery. We developed a simulation procedure to generate random treatment decentrations that present a distribution across a population based on from a recent clinical study [8].

Transition zone is important in modern laser algorithms for refractive surgery [10]. It connects the optical zone to the untreated cornea. The use of transition zone during LASIK resulted in a low incidence of postoperative glare and halos [11, 12]. Arbelaez *et al.* showed that a multidynamic aspheric transition zone was included in a cornea ablation profile in order to minimize the amount of induced optical aber-

Received June 16, 2013; revised ms. received August 20, 2013; published September 03, 2013 ISSN 1990-2573

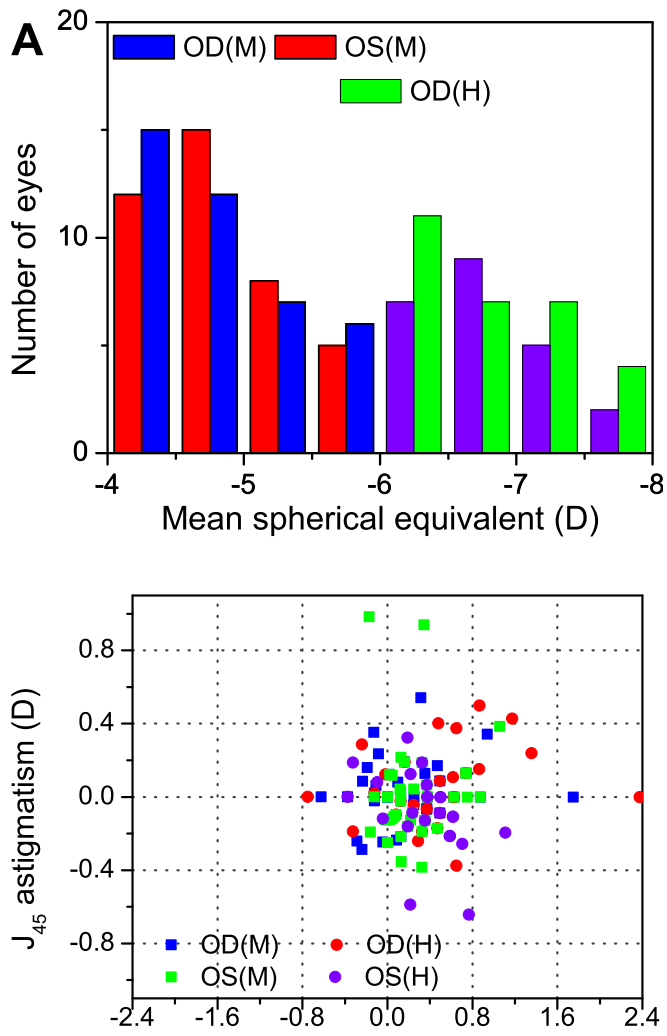

FIG. 1 Frequency distributions (OD=right eyes; OS=left eyes). M represents moderate myopia eyes, and H depicts high myopia eyes. A represents the spherical power of refractive error determined by the subjective refraction. B represents the astigmatism determined subjectively. N=132 eyes.

rations [13]. On the other hand, the pupil diameter exerted a great impact on wavefront aberration RMS. Applegate *et al.* revealed that the higher order aberration RMS increased rapidly with the pupil diameter increase in a normal population of human eyes [14]. Furthermore, several researches described the influence of pupil dilation on higher order aberrations after laser refractive surgery [15, 16]. For these reason, the effect of transition zone and pupil size on the postoperative aberrations would be considered in this theoretical analysis study.

Until now the theoretical comparison of residual wavefront aberrations after conventional and wavefront-guided refractive surgery with consideration of the both effect of decentration and transition zone has not been explicitly studied yet. In this paper, based on the corneal ablation profiles including transition zone, the residual wavefront aberrations with the effect of decentration were calculated. Additionally, the influence of oblique incidence on the residual aberrations was also taken into account.

2 MATERIALS AND METHODS

2.1 Subjects

In this study, 132 eyes of 74 potential laser refractive surgery candidates for myopia correction were enrolled. Patients with ocular disease, keratoconus, and previous ocular surgery were excluded. The age of the patients ranged from 18 to 34 years (mean, 24.4±4.9). The mean preoperative spherical power for the moderate and high myopia groups was -4.72±0.50D (range -4.00 to -5.75D) and -6.64±0.52D (range -6.00 to -7.75D), respectively, in left eyes. Also, the mean spherical power for the moderate and high myopia groups was -4.69±0.52D (range -4.00 to -5.75D) and -6.68± 0.58D (range -6.00 to -7.75D), respectively, in right eyes, with D representing diopter. Figure 1(a) shows the distribution of spherical power. In addition, the mean preoperative astigmatic power for the moderate and high myopia groups was -0.73±0.57D (from plano to -2.25D) and -0.97±0.50D (from -0.25 to -2.25D), respectively, in right eyes and -0.73±0.64D (from plano to -3.5D) and -1.21± 0.93D (from -0.25 to -4.75D), respectively, in left eyes, which is shown as a scatter plot of the orthogonal components J0 and J45 in Figure 1(b). The informed consent was obtained from all patients after an explanation of the procedure and its potential benefits and risks. The wavefront aberrations for all eyes were measured using a Shack-Hartmann aberrometer [17] (WaveScan wavefront system, VISX, Inc., Santa Clara, CA) in the scotopic condition. All measurements were repeated at least three times for each eye, and the 3 best-matching measurements were selected to be used. The wavefront aberration was fitted to Zernike polynomials up to sixth order. Then, the wavefront aberrations in a given diameter were computed by scaled transformation of Zernike aberrations. The contact lens wearers were excluded from this research.

2.2 Ablation profile for conventional and customized laser refractive surgery

In general, myopia and astigmatism components are generally included in the refractive errors in human eyes, namely myopia astigmatism. In the present study, when the anterior corneal surface is a spherical surface after refractive surgery, the ablation profile for conventional myopia astigmatism correction can be given by [18]:

$$\begin{aligned} D(x,y) = &\sqrt{(\sqrt{R_x^2 - x^2} + R_y - R_x)^2 - y^2} \\ &- \sqrt{R_f^2 - x^2 - y^2} + \sqrt{R_f^2 - (O/2)^2} \\ &+ R_x - R_y - \sqrt{R_x^2 - (O/2)^2} \end{aligned} \quad (1)$$

Here, R_x and R_y convey the radii of curvature of two principal meridians of the anterior corneal surface before refractive surgery. R_f depicts the postoperative radius of curvature. O is the diameter of optical zone in x-axis.

Clinically, the values of R_x, R_y, and R_f for myopia astigmatism correction in individual human eyes can be computed from the measured k value of cornea and the subjective refraction as [18].

On the other hand, according to the phase-conjugate principle, the ablation depth in optical zone for wavefront-guided myopia astigmatism correction can be given directly by wavefront information.

$$D(x,y) = -\sum_{\text{p and q}} W(x,y)/(n-1) \tag{2}$$

Here, n represents the refractive index of cornea in visible light, and the value is 1.376 in this paper. Also, (x,y) conveys an arbitrary point in optical zone on cornea. Additionally, the wavefront aberrations are expressed as a Zernike polynomial expansion.

$$W(x,y) = \sum_{\text{p and q}} c_p^q Z_p^q(x,y) \tag{3}$$

In this study, the ablation profile for transition zone should be structured. If ρ depicts the blend coefficient of ablation profile and R represents the radius of optical zone, the width of transition zone is $R\rho$. Here, the ablation profile for transition zone can be denoted as follows [19]:

$$D(x,y) = D_a(x,y)\cdot D_b(x,y) \quad R \le \sqrt{x^2+y^2} \le R(1+\rho) \tag{4}$$

Here, $D_a(x,y)$ indicates a blend function. Also, $D_b(x,y)$ conveys the extended ablation depth in transition zone, which is extended from the boundary value of optical zone.

2.3 Monte Carlo Simulating treatment decentration

In this research, the Monte Carlo simulation was performed for producing translation decentration. The decentration was randomly selected from a probability distribution across a population, which was obtained from a recent clinical study. For the moderate myopia eyes, the mean transverse translation in left and right eyes in the Monte Carlo analysis was 0.28±0.10 mm (range 0.10 to 0.46 mm) and 0.25±0.11 mm (range 0.07 to 0.47 mm), respectively (Figure 2). For the high myopia eyes, the mean translation in left and right eyes was 0.29±0.10 mm (range 0.10 to 0.50 mm) and 0.24±0.12 mm (range 0.08 to 0.51 mm), respectively.

2.4 Residual wavefront aberrations caused by treatment decentration

When decentration occurs, the actual ablation depth can be calculated by coordinate transformation. If a part of transition zone moves into pupil, the actual ablation depth should include two parts. One is the part that moves into pupil, which is computed from the transition zone, and then the other is a part of optical zone, which can be obtained from the ablation profile for optical zone. Then the Zernike coefficients can be achieved by surface fitting. In this section, the lateral decentration of ablation profile is explicitly considered. The coordinate transformation formula is given as follows:

$$\begin{aligned} x' &= (x-\Delta x) + (y-\Delta y) \\ y' &= (y-\Delta y) - (x-\Delta x) \end{aligned} \tag{5}$$

Here, Δx, Δy represent the lateral displacement in x- and y-axis, respectively. With coordinate transformation formula, the ablation depth in whole ablation zone can be calculated from the ablation profile. In addition, the ablation depth is multiplied by adjustment factors (κ) and then the effective depth can be obtained. Finally, the effective depth can be converted into the actual corrected aberrations:

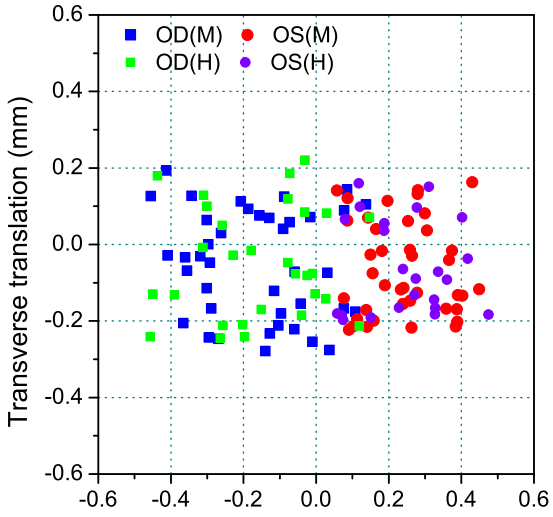

FIG. 2 Transverse translation (centration error) in 132 eyes (OD=right eyes; OS=left eyes). M represents moderate myopia eyes, and H depicts high myopia eyes.

$$W_d(x,y) = k\cdot D(x,y)\cdot(n-1) \tag{6}$$

The actual corrected Zernike coefficients can be given as follows:

$$W_d = \sum_{\text{p and q}} b_p^q Z_p^q(x,y) \tag{7}$$

Based on the ablation depth for conventional or wavefront-guided refractive surgery, we can obtain the actual corrected aberrations in a given pupil diameter. Then the Zernike coefficients of predicted residual aberrations after conventional or customized refractive surgery with treatment decentration can be calculated as follows:

$$W_r(x,y) = \sum_{\text{p and q}} a_p^q Z_p^q(x,y) + \sum_{\text{p and q}} b_p^q Z_p^q(x,y) \tag{8}$$

Here, b_q^p is the actual corrected Zernike coefficient with treatment decentration, and a_q^p is the coefficient of preoperative aberrations.

2.5 Comparison of residual wavefront aberrations

Based on the ablation profile for conventional and wavefront-guided refractive correction, the ablation depth for ablation zone including transition zone could be calculated. The distribution of translation of ablation centre was generated using Monte Carlo method. Additionally, the treatment decentration was simulated by coordinate transformation. Then the ablation depth was converted into the actual corrected aberrations. The residual aberrations were calculated as the differences between the original and actual corrected aberrations. Finally, the residual Zernike coefficients after conventional and customized laser refractive surgery were achieved by the surface fitting. In this paper, the comparison of residual aberrations after conventional and customized refractive surgery was performed for 5 mm, 6 mm and 7 mm pupil. Here, the

diameter of optical zone is 6 mm. In addition, the blend coefficient is 0.35, and then the diameter of ablation zone is 8.1 mm. In this section, the Zernike aberrations are expressed as the magnitude/axis form.

2.6 Comparison of optical quality

Stiles-Crawford effect (SCE) may have ability to compensate for the higher-order aberrations of the postoperative eyes and ameliorate the impacts of aberrations on visual performance when pupils are large [20]. In addition, visual performance after refractive surgery can be evaluated by an optical quality metric (VSMTF) based on modulation transfer function (MTF) [21, 22]. Consequently, the SCE can be modeled optically as a filter placed in front of the eye and incorporated into the point spread function and optical transfer function by introducing it into the pupil function. The visual Strehl ratio for MTF (VSMTF) is defined as the same in reference [21].

$$\mathrm{VSMTF} = \frac{\int_{-\infty}^{\infty}\int_{-\infty}^{\infty} \mathrm{CSF}_N(f_x,f_y)\mathrm{MTF}(f_x,f_y)df_xdf_y}{\int_{-\infty}^{\infty}\int_{-\infty}^{\infty} \mathrm{CSF}_N(f_x,f_y)\mathrm{MTF}_{DL}(f_x,f_y)df_xdf_y} \quad (9)$$

Here, CSF_N represents neural contrast sensitivity function, whereas MTF conveys the two-dimensional modulation transfer function influenced by both aberrations and SCE. $\mathrm{MTF}_D L$ is the diffraction-limited modulation transfer function. In this study, the MTF and VSMTF are calculated in a linear scale over the range of 0–60 cycles per degree. The comparison of optical quality after conventional and customized laser refractive surgery was performed for only 6 mm pupil.

3 RESULTS

3.1 Population statistics of the wavefront aberration

Figure 3 shows the average of the signed Zernike coefficients in a myopic population of 132 eyes (74 subjects) including mean value and standard deviation. The means of higher-order aberration RMS for moderate and high myopia eyes are 0.28 μm and 0.26 μm, respectively, in left eyes and 0.26 μm and 0.27 μm, respectively, in right eyes. However, spherical aberration is systematically biased toward positive values, and the mean coefficient for high myopia eyes is markedly larger than that for moderate myopia eyes. For example, the value of spherical aberration (C_4^0) RMS is all maximal being of 0.039 μm and 0.075 μm, respectively, in left eyes and 0.029 μm and 0.074 μm, respectively, in right eyes. The standard deviation of coma (C_3^{-1}) is maximal for moderate and high myopia eyes in left and right eyes. The mean standard deviations are 0.137, 0.158, 0.140 and 0.137, respectively. Note that distributions of aberrations for left and right eyes have similar means and variances.

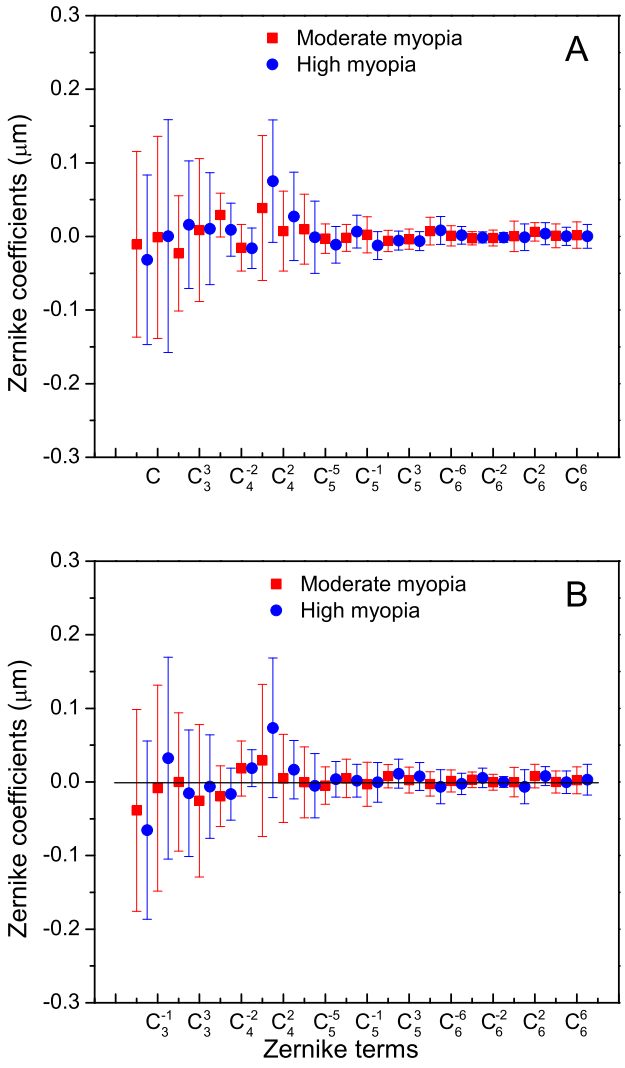

FIG. 3 Statistical summaries of Zernike coefficients for 132 eyes. The panel A corresponds to the OD (right eyes) and the panel B corresponds to OS (left eyes). Mean values of signed aberration coefficients are indicated by red squares for moderate myopia eyes and blue circles for high myopia eyes, with error bars indicating the standard deviations of the population. All aberration coefficients are in micrometers. Pupil diameter is 6 mm.

3.2 Comparison of residual aberrations after conventional and customized refractive surgery

Figure 4 shows the residual aberrations for a 5 mm pupil. The panel A corresponds to the right eyes (OD) and the panel B corresponds to the left eyes (OS).

The results in Figure 4 indicate that the residual aberration RMS is relatively small, and the mean coefficients are lower than 0.12 μm for all Zernike terms. However, the amount of residual aberrations for conventional correction is distinctly higher than that for customized correction. Especially, the residual coma, trefoil and spherical aberration are markedly larger than other aberration terms for conventional correction. Furthermore, the amounts of the residual fifth or sixth order aberrations are markedly lower than the second or third order aberrations. By comparison, the residual aberrations in left eyes show substantially the same as those in right eyes. It is worth noting that the main residual aberration term is coma. This result can be accounted by the clinical treatment decentration.

Figure 5 shows the residual aberrations for a 6 mm pupil. The panel A and panel B correspond to the right eyes (OD) and the left eyes (OS), respectively.

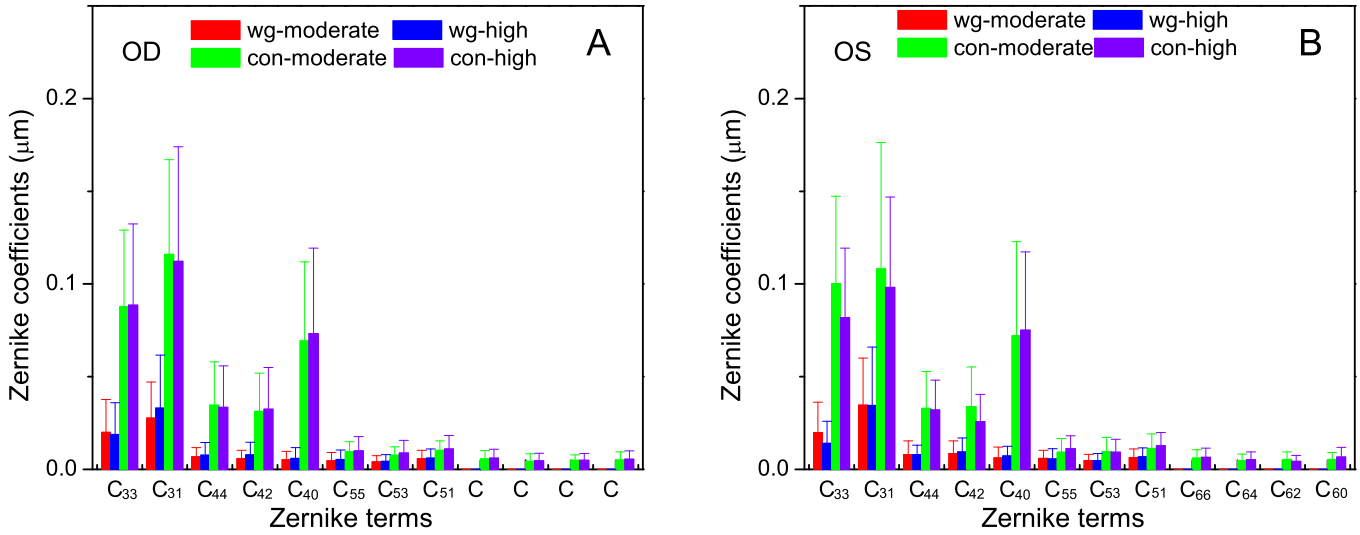

FIG. 4 Comparison of residual aberrations for conventional and customized correction with transition zone. The panel A corresponds to the right eyes (OD) and the panel B corresponds to the left eyes (OS). Mean values are indicated by red and blue columns for moderate and high myopia eyes after customized laser refractive surgery, respectively, with error bars indicating the standard deviations of the population. Also, mean values are indicated by green and violet columns for moderate and high myopia eyes after conventional refractive surgery, respectively. The diameter of optical zone is 6 mm, but the pupil diameter is 5 mm. The blend coefficient is 0.35 and the diameter of ablation zone reaches 8.1 mm.

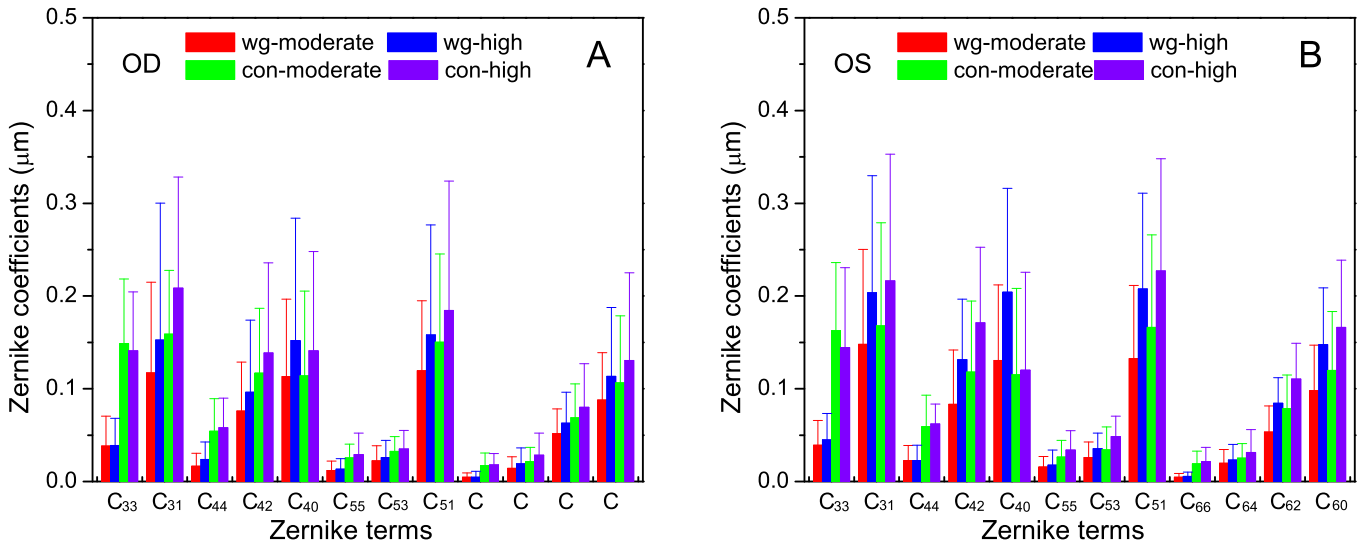

FIG. 5 Comparison of residual aberrations for conventional and customized correction with transition zone. The panel A corresponds to the right eyes (OD) and the panel B corresponds to the left eyes (OS). The diameter of pupil and optical zone is 6mm. The blend coefficient is 0.35 and the diameter of ablation zone is 8.1 mm.

The results in Figure 5 indicate that the amount of residual aberrations for conventional correction is also distinctly higher than that for customized correction. In addition, the residual aberrations for high myopia eyes are markedly larger than those for moderate myopia eyes. In this section, the significant residual aberration terms are trefoil, coma, secondary astigmatism, spherical aberration, secondary coma and secondary spherical aberration. By comparing conventional with customized correction, the residual aberrations for customized correction show slightly lower than those for conventional correction. It is worth noting that the amounts of the fifth and sixth order residual aberrations are relatively large, especially secondary coma. The mean RMS of secondary coma is larger than 0.12 μm; especially the value is 0.23 μm for high myopia eyes in left eyes after conventional correction.

Figure 6 shows the residual aberrations for a 7 mm pupil. It can be seen in Figure 6 that the amount of residual aberrations for high myopia eyes is markedly larger than that for moderate myopia eyes. Additionally, the residual aberrations for conventional correction are slight higher than those for customized correction. Furthermore, the amounts of residual the fifth and sixth order aberrations are relatively large (up to 0.83 μm) and yet they markedly lower than those of the third or fourth order aberrations. By comparing panel A with panel B, the residual aberrations in right eyes show slightly lower than those in left eyes. This result can be accounted by the differences in simulated decentration and refractive errors between the left and right eyes. It is worth noting that the main residual aberration term is spherical aberration. This result can be attributed to that the power of transition zone is less than that of optical zone, which will lead to the remains of some refractive errors and inducing spherical aberration.

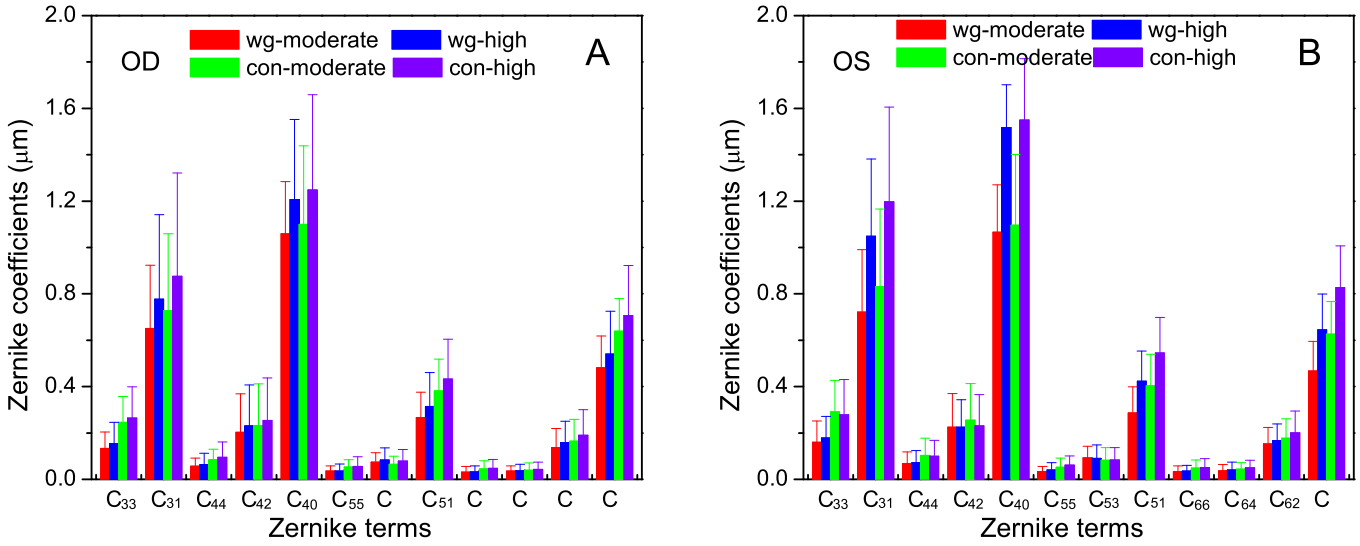

FIG. 6 Comparison of residual aberrations for conventional and customized correction with transition zone. The panel A corresponds to the right eyes (OD) and the panel B corresponds to the left eyes (OS). The diameter of optical zone is 6 mm, but the pupil diameter is 7 mm. The blend coefficient is 0.35.

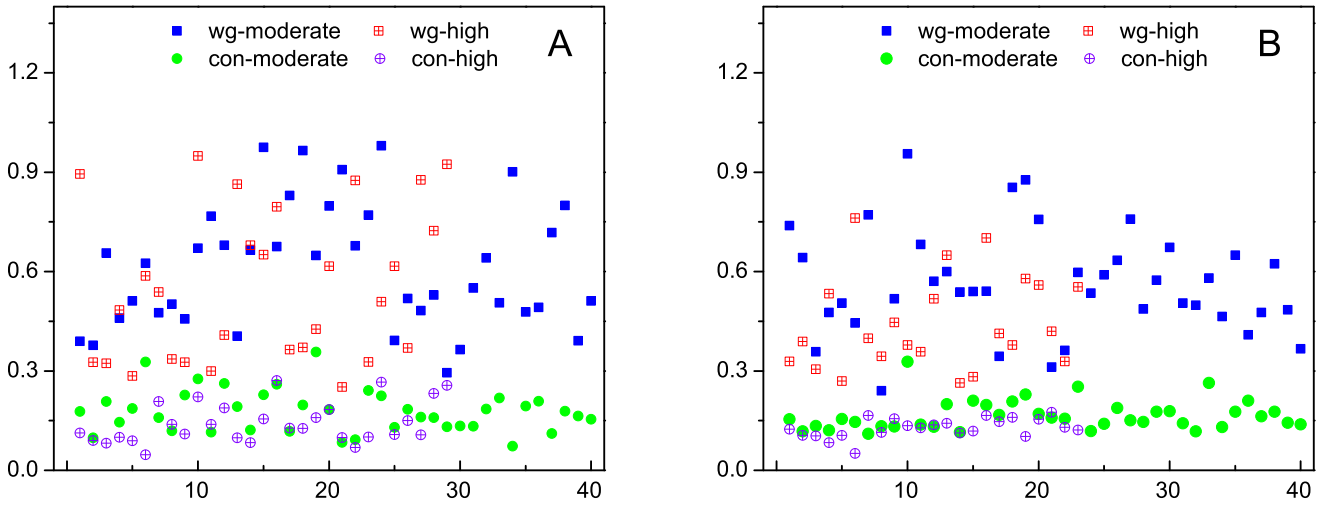

FIG. 7 Scatter plots of optical quality for conventional and customized correction with transition zone. The panel A corresponds to the right eyes (OD) and the panel B corresponds to the left eyes (OS). The diameter of pupil and optical zone is 6 mm.

3.3 Comparison of optical quality after conventional and customized refractive surgery

Figure 7 shows the optical quality for a 6 mm pupil after refractive surgery. The panel A corresponds to the right eyes (OD) and the panel B corresponds to the left eyes (OS). The results in Figure 7 indicate that the values of optical quality for customized correction are distinctly higher than those for conventional correction. In addition, the optical qualities for moderate myopia eyes are slightly higher than those for high myopia eyes. For the moderate myopia eyes, the predicted VSMTF values in left and right eyes for conventional correction will be lower 0.53±0.13 and 0.54±0.20 log unit than those for customized correction, respectively. For the high myopia eyes, the values of predicted optical quality in left and right eyes for conventional correction are lower 0.53±0.19 and 0.59±0.23 log unit than those for customized correction, respectively.

4 DISCUSSION

It is well known that the optical performance of human eye is dynamic. However, a fixed ablation center must be selected in laser refractive surgery. Generally, the entrance pupil center (EPC) is usually used as the ablation center in clinical practices and yet it changes with accommodation and the change of illumination [23]. Pupil centroid offset values are the factor most significantly correlated to the amount of treatment decentration. Therefore, ablation decentration may occur in laser refractive surgery due to pupil centroid shift in different illumination levels and the cyclotorsional change of the eye from seated to supine position. Ablation decentration plays an important role in inducing the optical aberrations and causing visual degradation. For example, ablation decentration >0.30 mm from the center of the entrance pupil is associated with greater induction of total HOA, coma, and spherical aberration after active eye-tracker-assisted myopic PRK, as compared with ablation decentration <0.15 mm. In addition, ablation decentration has a more significant in-

fluence on coma-inducing effects [24]. Bühren *et al.* found that pupil diameter and decentration explained up to 95% of the variance of VSOTF change after myopic photorefractive keratectomy (PRK) in a cat model [15]. Padmanabhan *et al.* revealed that eyes with decentered ablations had a significantly higher magnitude of induced aberrations and lower uncorrected visual acuity than eyes with well-centered ablations from wavefront-optimized ablation with an active eye tracker [9]. Bühren *et al.* indicated that center errors resulted in undercorrection of sphere and induction of astigmatism, and decentration mainly induced coma among the higher-order aberrations after photorefractive keratectomy (PRK) in a cat model [25]. Porter *et al.* reported that the mean shift in pupil center was 0.29 mm in wavefront-guided laser refractive surgery [26]. On the other hand, static cyclotorsion and dynamic cyclotorsion occurred during LASIK had been observed by Febbraro [27]. In our study, one limitation is that the cyclotorsional errors during refractive surgery are not considered.

Monte Carlo simulation is a standard computational technique and it may help predict the postoperative aberrations, for evaluating the consequences of refractive surgery in this analysis. We developed a simulation procedure to generate random translation decentration. Then, the amount of decentration of the eye was randomly selected from a probability distribution across a population. This simulation technique is not intended to a perfect representation of a single eye, but is developed for a correct distribution of the treatment decentration across a population. In a previous study, the Monte-Carlo method was employed for generating IOL decentration for evaluating the theoretical optical performance of 3 intraocular lens (IOL) designs in the presence of IOL decentration. The results indicated that this method was effective and practicable [28]. In addition, Canales *et al.* performed the simulation of the eye consisting of generation of random wavefronts that make up the ocular wave aberration statistics across a population by Monte Carlo method. They found that this method could be used to predict the performance of sensing techniques and to evaluate the consequences of customized ophthalmic elements and refractive surgery [29]. Furthermore, this approach was also used in predicting visual acuity from wavefront aberrations [30].

Some previous researches compared the induced aberrations and visual performance between conventional and wavefront-guided laser refractive surgery. Du *et al.* indicated that a statistically significant difference was noted in the increase of higher order aberrations after conventional and customized ablation in myopic LASIK [3]. In a comparison of night driving visual performance, the results showed that wavefront-guided LASIK to correct myopia significantly improved the mean performance and was significantly better than conventional LASIK for the treatment of moderate myopia [4]. In addition, wavefront-guided LASIK with iris-registration was efficient to reduce higher order aberrations especially coma and spherical aberrations, and to improve postoperative visual acuity and contrast sensitivity by comparison with conventional LASIK [6]. For the corneal topographic effective optical zone (EOZ) in eyes with spherical correction, wavefront-guided myopic LASIK increased the postoperative EOZ, but standard LASIK decreased EOZ [7]. It deserved to note that different laser platforms achieved statistically significantly different visual performance and induced higher-order aberrations [31]. Furthermore, pupil size exerted a crucial impact on the wavefront aberration RMS [32]. Additionally, the diameter of pupil and optical zone is usually inconsistent in clinical practices. Our results are sufficient to support the conclusion drawn by Bühren *et al.* that the optical zone to pupil ratio had a significant impact on higher-order aberrations induction after refractive surgery [16]. Because an abrupt change in corneal curvature may induce excessive epithelial and the haze may be confined to the wound edge, the transition zone must be included in the modern refractive surgery. Corneal postoperative optical aberrations with a larger ablation zone including transition zone were less pronounced than those associated with no transition zone [33]. Additionally, our results demonstrated that the ablation profile with transition zone may account for a main portion of the increase of postoperative higher-order aberrations, especially coma and spherical aberrations [34, 35]. Furthermore, the regularity in ablation area could be improved by final smoothing, which may improve the optical and functional outcomes of laser refractive surgery [36, 37]. In this study, the ablation profile of transition zone, treatment decentration and pupil diameter were all the same in this simulation analysis, and this may mirror the differences of outcomes between conventional and customized correction.

5 CONCLUSION

For preoperative optical aberrations, the distributions showed the similar means and variances in left and right eyes. In addition, the mean of residual spherical aberration for high myopia eyes was markedly larger than that for moderate myopia eyes. According to the ablation profile with transition zone, the residual optical aberrations after conventional and customized laser refractive surgery were compared. The results indicated that the amount of residual aberrations for conventional correction was higher than that for customized correction. Additionally, the residual aberrations for high myopia eyes were markedly larger than those for moderate myopia eyes. For a 5 mm pupil, the main residual aberration term was coma. However, the significant aberration term was spherical aberration for a 7 mm pupil. It was worth noting that the magnitudes of the residual fifth or sixth order aberrations were relatively large, especially secondary coma for a 6 mm pupil and secondary spherical aberration for a 7 mm pupil, namely, when the pupil diameter was the same as optical zone or greater. Furthermore, the values of optical quality for customized correction are higher than those for conventional correction. Our results demonstrated that the customized ablation profile may be superior to the conventional correction. However, the customized ablation profile may still induce significant amount of residual aberrations. Therefore, new ablation algorithm is needed to fix the spherical aberration induced from the conventional Munnerlyn shape and the eye tracking during ablation is important to reduce residual aberrations. Clinically, it is not necessary to select the customized ablation profile for those of human eyes with normal levels of preoperative aberration.

6 ACKNOWLEDGEMENTS

This research is supported by the National Natural Science Foundation of China (No. 81170873) and the science and technology funds from Jiangxi Education Department (No. GJJ12409).

References

[1] F. Wu, Y. Yang, and P. J. Dougherty, "Contralateral comparison of wavefront-guided LASIK surgery with iris recognition versus without iris recognition using the MEL80 Excimer laser system," Clin. Exp. Optom. **92**, 320–327 (2009).

[2] S. C. Schallhorn, and J. A. Venter, "One-month outcomes of wavefront-guided LASIK for low to moderate myopia with the VISX STAR S4 laser in 32,569 eyes," J. Refract. Surg. **25**, S634–S641 (2009).

[3] C. X. Du, Y. Shen, and Y. Wang, "Comparison of high order aberration after conventional and customized ablation in myopic LASIK in different eyes of the same patient," J. Zhejiang. Univ. Sci. B **8**, 177–180 (2007).

[4] S. C. Schallhorn, D. J. Tanzer, S. E. Kaupp, M. Brown and S. E. Malady, "Comparison of night driving performance after wavefront-guided and conventional LASIK for moderate myopia," Ophthalmology **116**, 702–709 (2009).

[5] S. T. Awwad, K. K. Haithcock, D. Oral, R. W. Bowman, H. D Cavanagh and J. P McCulley, "A comparison of induced astigmatism in conventional and wavefront-guided myopic LASIK using LADARVision4000 and VISX S4 platforms," J. Refract. Surg. **21**, S792–S798 (2005).

[6] J. Zhang, Y. H. Zhou, N. L. Wang, and R. Li, "Comparison of visual performance between conventional LASIK and wavefront-guided LASIK with iris-registration," Chin Med J (Engl) **121**, 137–142 (2008).

[7] L. Racine, L. Wang, and D. D. Koch, "Size of corneal topographic effective optical zone: comparison of standard and customized myopic laser in situ keratomileusis," Am. J. Ophthalmol. **142**, 227–232 (2006).

[8] L. Wang, and D. D. Koch, "Residual higher-order aberrations caused by clinically measured cyclotorsional misalignment or decentration during wavefront-guided excimer laser corneal ablation," J. Cataract. Refract. Surg. **34**, 2057–2062 (2008).

[9] P. Padmanabhan, M. Mrochen, D. Viswanathan, and S. Basuthkar, "Wavefront aberrations in eyes with decentered ablations," J. Cataract Refract. Surg. **35**, 695–702 (2009).

[10] S. MacRae, "Excimer ablation design and elliptical transition zones," J. Cataract Refract. Surg. **25**, 1191–1197 (1999).

[11] M. S. Macsai, K. Stubbe, A. P. Beck, and Z. B. Ravage, "Effect of expanding the treatment zone of the Nidek EC-5000 laser on laser in situ keratomileusis outcomes," J. Cataract Refract. Surg. **30**, 2336–2343 (2004).

[12] M. A. el Danasoury, "Prospective bilateral study of night glare after laser in situ keratomileusis with single zone and transition zone ablation," J. Refract. Surg. **14**, 512–516 (1998).

[13] M. C. Arbelaez, C. Vidal, B. A. Jabri, and S. Arba Mosquera, "LASIK for myopia with Aspheric 'aberration neutral' ablations using the ESIRIS laser system," J. Refract. Surg. **25**, 991–999 (2009).

[14] R. A. Applegate, W. J. Donnelly, J. D. Marsack, and D. E. Koenig, "Three-dimensional relationship between high-order root-mean-square wavefront error, pupil diameter, and aging," J. Opt. Soc. Am. A Opt. Image Sci. Vis. **24**, 578–587 (2007).

[15] J. Bühren, G. Yoon, S. MacRae, and K. Huxlin, "Contribution of optical zone decentration and pupil dilation on the change of optical quality after myopic photorefractive keratectomy in a cat model," J. Refract. Surg. **26**, 183–190 (2010).

[16] J. Bühren, C. Kuhne, and T. Kohnen, "Influence of pupil and optical zone diameter on higher-order aberrations after wavefront-guided myopic LASIK," J. Cataract Refract. Surg. **31**, 2272–2280 (2005).

[17] J. Liang, B. Grimm, S. Goelz, and J. F. Bille, "Objective measurement of wave aberrations of the human eye with the use of a Hartmann-Shack wave-front sensor," J. Opt. Soc. Am. A Opt. Image Sci. Vis. **11**, 1949–1957 (1994).

[18] L. Fang, X. He, and F. Chen, "Theoretical analysis of wavefront aberration from treatment decentration with oblique incidence after conventional laser refractive surgery," Opt. Express **18**, 22418–22431 (2010).

[19] Y. Zhang, W. Liao, and J. Shen, "Blend zone model for excimer laser refractive surgery," Opt. Precision Eng. **12**, 406–410 (2004).

[20] L. Fang, Y. Wang, and F. Chen, "Influence of Stiles-Crawford effect on visual performance after laser in situ keratomileusis," J. Opt. Soc. Am. A Opt. Image Sci. Vis. **29**, 1482–1488 (2012).

[21] L. N. Thibos, X. Hong, A. Bradley, and R. A. Applegate, "Accuracy and precision of objective refraction from wavefront aberrations," J. Vis. **4**, 329–351 (2004).

[22] J. D. Marsack, L. N. Thibos, and R. A. Applegate, "Metrics of optical quality derived from wave aberrations predict visual performance," J. Vis. **4**, 322–328 (2004).

[23] L. Wu, X. Zhou, R. Chu, and Q. Wang, "Photoablation centration on the corneal optical center in myopic LASIK using A0V excimer laser," Eur. J. Ophthalmol. **19**, 923–929 (2009).

[24] S. B. Lee, B. S. Hwang, and J. Lee, "Effects of decentration of photorefractive keratectomy on the induction of higher order wavefront aberrations," J. Refract. Surg. **26**, 731–743 (2010).

[25] J. Bühren, G. Yoon, S. Kenner, S. MacRae, and K. Huxlin, "The effect of optical zone decentration on lower- and higher-order aberrations after photorefractive keratectomy in a cat model," Invest. Ophthalmol. Vis. Sci. **48**, 5806–5814 (2007).

[26] J. Porter, G. Yoon, D. Lozano, J. Wolfing, R. Tumbar, S. MacRae, I. G. Cox, and D. R. Williams, "Aberrations induced in wavefront-guided laser refractive surgery due to shifts between natural and dilated pupil center locations," J. Cataract Refract. Surg. **32**, 21–32 (2006).

[27] J. L. Febbraro, D. D. Koch, H. N. Khan, A. Saad, and D. Gatinel, "Detection of static cyclotorsion and compensation for dynamic cyclotorsion in laser in situ keratomileusis," J. Cataract Refract. Surg. **36**, 1718–1723 (2010).

[28] G. E. Altmann, L. D. Nichamin, S. S. Lane, and J. S. Pepose, "Optical performance of 3 intraocular lens designs in the presence of decentration," J. Cataract Refract. Surg. **31**, 574–585 (2005).

[29] V. F. Canales, and M. P. Cagigal, "Monte Carlo simulation of irradiance distribution on the retina after refractive surgery," J. Refract. Surg. **20**, 384–390 (2004).

[30] A. B. Watson, and A. J. Ahumada, Jr., "Predicting visual acuity from wavefront aberrations," J. Vis. **8**, 17, 1–19 (2008).

[31] P. S. Binder, and J. Rosenshein, "Retrospective comparison of 3 laser platforms to correct myopic spheres and spherocylinders using conventional and wavefront-guided treatments," J. Cataract Refract. Surg. **33**, 1158–1176 (2007).

[32] G. M. Dai, "Scaling Zernike expansion coefficients to smaller pupil sizes: a simpler formula," J. Opt. Soc. Am. A Opt. Image Sci. Vis. **23**, 539–543 (2006).

[33] M. J. Endl, C. E. Martinez, S. D. Klyce, M. B. McDonald, S. J. Coorpender, R. A. Applegate and H. C. Howland, "Effect of larger ablation zone and transition zone on corneal optical aberrations after photorefractive keratectomy," Arch. Ophthalmol. **119**, 1159–1164 (2001).

[34] M. Mrochen, M. Kaemmerer, P. Mierdel, and T. Seiler, "Increased higher-order optical aberrations after laser refractive surgery: a problem of subclinical decentration," J. Cataract Refract. Surg. **27**, 362–369 (2001).

[35] Y. Wang, K. X. Zhao, J. C. He, Y. Jin, and T. Zuo, "Ocular higher-order aberrations features analysis after corneal refractive surgery," Chin. Med. J. (Engl) **120**, 269–273 (2007).

[36] P. Vinciguerra, M. Azzolini, P. Airaghi, P. Radice, and V. de Molfetta, "Effect of decreasing surface and interface irregularities after photorefractive keratectomy and laser in situ keratomileusis on optical and functional outcomes," J. Refract Surg. **14**, S199–S203 (1998).

[37] P. Vinciguerra, F. I. Camesasca, and I. M. Torres, "Transition zone design and smoothing in custom laser-assisted subepithelial keratectomy," J. Cataract Refract. Surg. **31**, 39–47 (2005).